Inorg. Chem. **1995,** *34,* 6430−6439

Palladium-Assisted Cyano Substitution Reactions of $(PMe_2Ph)_2Pd(B_9H_9As_2)$ and $(PMe_2Ph)_2Pd(B_9C_2H_{11})$. X-ray Crystal and Molecular Structures of 5-CN-1,1-$(PMe_2Ph)_2$-*closo*-1,2,3-$PdAs_2B_9H_8$, 1-^{t}BuNC-5-CN-1-(PMe_2Ph)-*closo*-1,2,3-$PdAs_2B_9H_8$, and 4,5-$(CN)_2$-1,1-$(PMe_2Ph)_2$-*closo*-1,2,3-$PdC_2B_9H_9$

Steve A. Jasper, Jr., John C. Huffman, and Lee J. Todd*

Department of Chemistry and Molecular Structure Center, Indiana University,
Bloomington, Indiana 47405

Received April 14, 1995⊗

The reaction of 1,1-$(PMe_2Ph)_2$-*closo*-1,2,3-$PdAs_2B_9H_9$ (**A**) with ^{t}BuNC formed low yields of 5-CN-1,1-$(PMe_2Ph)_2$-*closo*-1,2,3-$PdAs_2B_9H_8$ (**2**) and/or 1-^{t}BuNC-5-CN-1-(PMe_2Ph)-*closo*-1,2,3-$PdAs_2B_9H_8$ (**3**). The use of $(^tBuNC)_2PdCl_2$ as a reagent in this reaction gave an improved yield of compound **3**. Similar reaction of 1,1-$(PMe_2Ph)_2$-*closo*-1,2,3-$PdC_2B_9H_{11}$ (**4**) with $(^tBuNC)_2PdCl_2$ gave 4,5-$(CN)_2$-1,1-$(PMe_2Ph)_2$-*closo*-1,2,3-$PdC_2B_9H_9$ (**5**). Reaction of **A** with $(PMe_2Ph)_2P(CN)_2$ gave 1-CN-1,5-$(PMe_2Ph)_2$-*closo*-1,2,3−$PdAs_2B_9H_8$ (**1**) in low yield. Compounds **2**, **3**, and **5** were characterized by X-ray diffraction studies. Compound **2** consisted of bright purple crystals of monoclinic space group $P2_1/n$, with a = 12.460(2) Å, b = 11.583(2) Å, c = 19.114(4) Å, β = 107.31(1)°, and Z = 4. The structure was determined by conventional heavy-atom methods and refined to a final value of R = 0.0432 (3899 reflections) and R_w = 0.0458. Compound **3** consisted of magenta plates with triclinic space group $P\bar{1}$, with a = 11.586(3) Å, b = 11.813(3) Å, c = 9.799(2) Å, α = 95.33(1)°, β = 114.58(1)°, γ = 80.17(1)°, and Z = 2. The structure was determined by conventional heavy-atom methods and refined to a final value of R = 0.0235 (3323 reflections), R_w = 0.0245. Compound **5** consisted of red needles with monoclinic space group $P2_1/n$, with a = 10.383(2) Å, b = 18.875(3) Å, c = 13.682(2) Å, β = 105.41(1)°, and Z = 4. The structure was determined by conventional heavy-atom methods and refined to a final value of R = 0.0362 (3547 reflections), R_w = 0.0335.

Introduction

We have recently investigated two areas of research, that of metalladiarsaboranes,[1] and that of palladium-assisted substitution reactions of some common borane anions.[2] These investigations have now merged into a more general study of various types of cage substitution reactions.

The starting points for the immediate reactions were the compounds $(PMe_2Ph)_2Pd(B_9H_9As_2)$, reported earlier, and $(PMe_2Ph)_2Pd(B_9C_2H_{11})$, which is a new compound, but which is closely related to the known $(PMe_3)_2Pd(B_9C_2H_{11})$, $[P(OMe)_3]_2Pd(B_9C_2H_{11})$, (dppe)$Pd(B_9C_2H_{11})$,[3] and the recently reported $(PMe_2Ph)_2Pd(B_9C_2Me_2H_9)$.[4] In addition, two substituted palladacarborane derivatives were recently reported, $(\eta^2,\sigma$-5-OMe-$C_8H_{12})Pd(4$-SMe_2-$B_9C_2H_{10})$ and $[(cod)Pd(4$-SMe_2-$B_9C_2H_{10})][BF_4]$.[5]

We have shown that reaction of $(PMe_2Ph)_2Pd(B_9H_9As_2)$ with $(PMe_2Ph)_2PdCl_2$ gives 1,6-Cl_2-1,5-$(PMe_2Ph)_2$-*closo*-1,2,3-$PdAs_2B_9H_7$ as one of the products.[1] Thus halogens and phosphines appear to participate in palladium-mediated substitution. To investigate the possibility that the pseudohalogen cyanide can substitute via palladium mediation, we reacted $(PMe_2Ph)_2Pd(B_9H_9As_2)$ with $(PMe_2Ph)_2P(CN)_2$ and also with ^{t}BuNC. We also reacted $(PMe_2Ph)_2Pd(B_9H_9As_2)$ and $(PMe_2Ph)_2Pd(B_9C_2H_{11})$ with $(^tBuNC)_2PdCl_2$. Herein we report upon palladium-assisted cyano substitution reactions and several new palladaheteroborane complexes that were isolated from these reactions.

Experimental Section

Physical Measurements. Boron (^{11}B) NMR spectra were obtained at 115.85 MHz (21 °C) with a Nicolet NT-360 spectrometer and were externally referenced to BF_3·OEt_2. Phosphorus (^{31}P) NMR were obtained at 146.2 MHz (21 °C) and externally referenced to 85% H_3PO_4. Proton (^{1}H) spectra were obtained at 361.1 MHz (21 °C) and internally referenced to $CHCl_3$. In all NMR spectra, positive chemical shifts were downfield. Infrared spectra were obtained as KBr pellets and recorded on a Nicolet 510P Fourier transform spectrometer. Melting points were obtained in sealed, evacuated capillaries and are uncorrected. Elemental analyses were performed by Schwarzkopf Microanalytical Laboratories, Woodside, NY.

Materials. All reactions were performed under an atmosphere of prepurified nitrogen. Tetrahydrofuran (THF) was freshly distilled from sodium benzophenone ketyl. The palladadiarsaborane 1,1-$(PMe_2Ph)_2$-*closo*-1,2,3-$PdAs_2B_9H_9$[1] and the carborane $[Me_3NH]$[*nido*-7,8-$C_2B_9H_{12}$][6] were prepared by previous literature methods. The palladium reagent $(PMe_2Ph)_2Pd(CN)_2$ was prepared by cyanide metathesis with the chloro analogue, by the method of Nelson et al.[7,8] The palladium reagent

---

⊗ Abstract published in *Advance ACS Abstracts,* October 1, 1995.

(1) Jasper, S. A., Jr.; Roach, S.; Stipp, J. N.; Huffman, J. C.; Todd, L. J. *Inorg. Chem.* **1993**, 32, 3072.

(2) Jasper, S. A., Jr.; Jones, R. B.; Mattern, J.; Huffman, J. C.; Todd, L. J. *Inorg. Chem.* **1994**, 33, 5620.

(3) Colquhoun, H. M.; Greenhough, T. J.; Wallbridge, M. G. H. *J. Chem. Soc., Dalton Trans.* **1985**, 761.

(4) Fallis, K. A.; Mullica, D. F.; Sappenfield, E. L.; Stone, F. G. A. *Inorg. Chem.* **1994**, 33, 4927.

(5) Bouek, N. L.; Welch, A. J. *J. Chem. Soc., Dalton Trans.* **1993**, 1917.

(6) Plesek, J.; Hermanek, S.; Stibr, B.; *Inorg. Synth.* **1983**, 22, 231.

(7) Rahn, J. A.; O'Donnell, D. J.; Palmer, A. R.; Nelson, J. H. *Inorg. Chem.* **1989**, 28, 2631.

0020-1669/95/1334-6430$09.00/0

(^{t}BuNC)$_2$PdCl$_2$ was prepared by the method of Otsuka et al.[9] All other commercially available reagents were used as purchased.

1-CN-1,5-(PMe$_2$Ph)$_2$-*closo*-1,2,3-PdAs$_2$B$_9$H$_8$ (1). In a two-neck round-bottom flask equipped with a stir bar, septum, and nitrogen inlet were placed (PMe$_2$Ph)$_2$Pd(B$_9$H$_9$As$_2$) (65 mg, 0.10 mmol), (PMe$_2$Ph)$_2$Pd(CN)$_2$ (43 mg, 0.10 mmol), and 8 mL of THF. The septum was replaced with a condenser, and the solution was brought to reflux for 6 h, after which the THF was removed under reduced pressure. The remaining solids were redissolved in approximately 5 mL of CH$_2$Cl$_2$, and 1 g of silica gel (Merck grade 60, 230–400 mesh, 60 Å) was added. The CH$_2$Cl$_2$ was removed under reduced pressure and the solids were packed on a 23 cm × 1.0 cm silica gel chromatography column and eluted with 1:1 (v/v) toluene:CH$_2$Cl$_2$. The major fraction was red, with $R_f = 0.05$ by TLC (CH$_2$Cl$_2$ mobile phase, Ag$^+$ development). The solvents were stripped off, the solids were redissolved in CH$_3$CN and filtered through glass wool, and the CH$_3$CN from the filtrate was removed *in vacuo* (17.4 mg, 26.5% yield). Anal. Calcd for C$_{17}$H$_{30}$As$_2$B$_9$NP$_2$Pd: C, 30.75; H, 4.55. Found: C, 30.84; H, 4.54.

5-CN-1,1-(PMe$_2$Ph)$_2$-*closo*-1,2,3-PdAs$_2$B$_9$H$_8$ (2). In a two-neck round-bottom flask equipped with a stir bar, septum, and nitrogen inlet were placed (PMe$_2$Ph)$_2$Pd(B$_9$H$_9$As$_2$) (149 mg, 0.233 mmol) and 10 mL of dry THF. Then, *tert*-butyl isocyanide (0.054 mL, 0.48 mmol) was added via syringe. The mixture was heated to reflux for 15 h, during which the solution changed from red-purple to red-brown. The THF was removed by rotary evaporation, and approximately 5 mL of CH$_2$Cl$_2$ and 2 g of silica gel (Merck grade 60, 230–400 mesh) were added. The CH$_2$Cl$_2$ was removed under reduced pressure, and the remaining solids were packed on a 40 cm x 2.4 cm silica gel chromatography column and eluted with 1:1 (v/v) toluene:CH$_2$Cl$_2$. There were two principal bands: the more nonpolar was unreacted starting material, with $R_f = 0.8$ by TLC (CH$_2$Cl$_2$ mobile phase, Ag$^+$ development); the more polar was electric purple, with $R_f = 0.2$. A similarly equipped reaction was performed, with the following changes: 300 mg (0.470 mmol) of (PMe$_2$Ph)$_2$Pd(B$_9$H$_9$As$_2$) and 15 mL of THF were used; 1.75 mL (15.5 mmol) *tert*-butyl isocyanide was added over 4 days of heating to reflux. The purple bands from both reactions were combined, and recrystallization from CH$_2$Cl$_2$/hexanes yielded bright purple crystals (37 mg, 7.9% combined yield for both reactions).

1-^{t}BuNC-5-CN-1-(PMe$_2$Ph)-*closo*-1,2,3-PdAs$_2$B$_9$H$_8$ (3). In a two-neck round-bottom flask equipped with a stir bar, septum, and nitrogen inlet were placed (PMe$_2$Ph)$_2$Pd(B$_9$H$_9$As$_2$) (129 mg, 0.201 mmol), (^{t}BuNC)$_2$PdCl$_2$ (70 mg, 0.204 mmol), and 8 mL of THF. The septum was replaced by a condenser, and a heating mantle was used to bring the solution to reflux for 3 days, after which the THF was removed under reduced pressure. The remaining solids were redissolved in approximately 5 mL of CH$_2$Cl$_2$, and 1 g of silica gel (Merck grade 60, 230–400 mesh, 60 Å) was added. The CH$_2$Cl$_2$ was removed under reduced pressure, and the solids were packed on a 29 cm × 1.0 cm silica gel chromatography column and eluted with 1:1 toluene:CH$_2$Cl$_2$. The major fraction was magenta, with $R_f = 0.25$ by TLC (CH$_2$Cl$_2$ mobile phase, Ag$^+$ development). The solvents were stripped off, and the solids were recrystallized from CH$_2$Cl$_2$/pentane at room temperature (34.8 mg, 28.3% yield). Anal. Calcd for C$_{14}$H$_{28}$As$_2$B$_9$N$_2$PPd: C, 27.61; H, 4.63. Found: C, 27.94; H, 4.60.

1,1-(PMe$_2$Ph)$_2$-*closo*-1,2,3-PdC$_2$B$_9$H$_{11}$ (4). In a two-neck round-bottom flask equipped with a stir bar, septum, and nitrogen inlet was placed [Me$_3$NH][*nido*-7,8-C$_2$B$_9$H$_{12}$] (1.878 g, 9.704 mmol). Dry THF (20 mL) was added via syringe, to dissolve the solid, followed by *n*-butyllithium (24.4 mmol = 2.51 equiv) in hexanes solution, dropwise. The solution became slightly yellow and slightly cloudy, and significant heat evolution was observed. After 15 min of stirring, the THF and Me$_3$N were removed *in vacuo*, to leave a gooey white solid. The solids were then redissolved in THF (60 mL), and PdCl$_2$(PMe$_2$Ph)$_2$ (4.402 g, 9.704 mmol) was added directly to the reaction mixture under N$_2$ purge. The solution quickly turned yellow-orange. After 2.5 h, the THF was removed *in vacuo*, the solids were redissolved in a minimum amount of CH$_2$Cl$_2$, and approximately 2 g of silica gel (60 Å, 230–400 mesh) was added. The CH$_2$Cl$_2$ was removed *in vacuo*, and the solids were packed on a 38 cm x 2.4 cm silica gel chromatography column and eluted with 1:1 (v/v) toluene:CH$_2$Cl$_2$, followed by CH$_2$Cl$_2$. There were two principal bands: band I was amber, with $R_f = 0.50$ by TLC (toluene mobile phase); band II was red-purple, with $R_f = 0.40$. The solvents were stripped off and the solids maintained under a N$_2$ atmosphere. Band I was determined by ^{11}B NMR to be 9-PMe$_2$Ph-*nido*-7,8-C$_2$B$_9$H$_{11}$.[10] Band I was recrystallized from CH$_2$Cl$_2$/pentane at 5 °C, to yield yellow needles of varying sizes (total of 4 crops: 255 mg, 9.71% yield). Band II was crystallized from CH$_2$Cl$_2$/pentane at 5 °C, to yield red rectangular crystals of varying sizes (total of 6 crops: 491 mg, 9.82% yield). Mp: 117–124 °C dec.

4,5-(CN)$_2$-1,1-(PMe$_2$Ph)$_2$-*closo*-1,2,3-PdC$_2$B$_9$H$_9$ (5). In a two-neck round-bottom flask equipped with a stir bar, septum, and nitrogen inlet were placed (PMe$_2$Ph)$_2$Pd(B$_9$C$_2$H$_{11}$) (206 mg, 0.400 mmol), (^{t}BuNC)$_2$PdCl$_2$ (137 mg, 0.399 mmol), and 15 mL of THF. The septum was replaced with a water condenser, and the solution was brought to reflux for 8 h, after which the solution was filtered on a coarse frit and the THF was removed under reduced pressure. The remaining solids were redissolved in approximately 5 mL of CH$_2$Cl$_2$, and 1 g of silica gel (Merck grade 60, 230–400 mesh, 60 Å) was added. The CH$_2$Cl$_2$ was removed under reduced pressure, and the solids were packed on a 36 cm × 2.4 cm silica gel chromatography column. Gradient elution with 1:1 (v/v) toluene:CH$_2$Cl$_2$, followed by CH$_2$Cl$_2$, and 8:1 (v/v) CH$_2$Cl$_2$:CH$_3$CN yields four principal bands. Band I was yellow, with $R_f = 0.92$ by TLC (CH$_2$Cl$_2$ mobile phase, Ag$^+$ development) and was identified as a mixture of isomers of PMe$_2$Ph-*nido*-7,8-C$_2$B$_9$H$_{11}$ by ^{11}B NMR (17 mg, 16% yield). Band II was red, with $R_f = 0.82$, and was identified as unreacted starting material by ^{11}B NMR (14 mg, 6.8% recovered unreacted). Band III had $R_f = 0.33$ and remains an uncharacterized product. Band IV had $R_f = 0.05$ and was identified as **5**. The solvents were stripped off, and the solids were maintained under a N$_2$ atmosphere. Band IV was crystallized from CH$_2$Cl$_2$/pentane by diffusion at room temperature to yield red needles (29 mg, 13% yield).

Crystal Structure Determinations. The diffractometer utilized for data collection was designed and constructed locally. A Picker four-circle goniostat equipped with a Furnas monochromator (HOG crystal) and Picker X-ray generator was interfaced to a Z80 microprocessor which was controlled by an RS232 serial port on an IBM PC microcomputer. Motors were slo-syn stepping motors, and a special top/bottom–left/right slit assembly was used to align each crystal. All computations were performed on IBM compatible microcomputer systems using DOS or OS/2 operating systems.

For **2**, **3**, and **5**, data were collected using standard moving crystal–moving detector technique. A continuous θ, 2θ scan technique with fixed backgrounds at each extreme of the scan was employed (see Table 15 for complete unit cell parameters). A well-formed purple crystal of (PMe$_2$Ph)$_2$Pd(5-CN-B$_9$H$_8$As$_2$) (**2**) with dimensions 0.25 × 0.25 × 0.25 mm was affixed to the end of a glass fiber using silicone grease and transferred to the goniostat where it was cooled to −166 °C for characterization and data collection. A small well-formed fragment of a larger magenta crystal of (^{t}BuNC)(PMe$_2$Ph)Pd(5-CN-B$_9$H$_8$As$_2$) (**3**) with dimensions 0.12 × 0.22 × 0.24 mm, was affixed to the end of a glass fiber using silicone grease and transferred to the goniostat where it was cooled to −172 °C for characterization and data collection. A well-formed red needle of (PMe$_2$Ph)$_2$Pd(4,5-(CN)$_2$-B$_9$C$_2$H$_9$) (**5**) was cleaved to form a smaller fragment with dimensions 0.20 × 0.25 × 0.40 mm, which was affixed to the end of a glass fiber using silicone grease and transferred to the goniostat where it was cooled to −175 °C for characterization and data collection.

A systematic search of a limited hemisphere of reciprocal space revealed a set of diffraction maxima with symmetry and systematic absences corresponding to the unique monoclinic space group $P2_1/n$ for **2** and **5**. For **3**, a set of diffraction maxima with no symmetry or systematic absences was located, indicating a triclinic space group. Subsequent solution and refinement confirmed these choices. Data were corrected for Lorentz and polarization effects. For **2** and **5**, equivalent data were averaged to yield a final unique set of intensities. For **3**, an absorption correction was made based on the size of the crystal.

---

(8) Roberts, N. K.; Skelton, B. W.; White, A. H.; Wild, S. B. *J. Chem. Soc., Dalton Trans.* **1982**, 2093.

(9) Otsuka, S.; Tatsuno, Y.; Ataka, K. *J. Am. Chem. Soc.* **1971**, 93, 6705.

(10) Kim, K. M.; Do, Y.; Knobler, C. B.; Hawthorne, M. F. *Bull. Korean Chem. Soc.* **1989**, 10, 321.

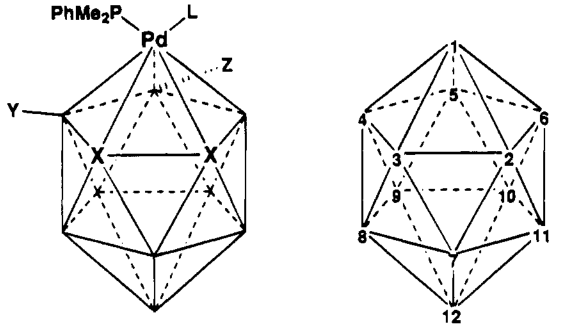

	X	Y	Z	L
A	As	H	H	PMe_2Ph
1	As	H	PMe_2Ph	CN
2	As	H	CN	PMe_2Ph
3	As	H	CN	^{t}BuNC
4	CH	H	H	PMe_2Ph
5	CH	CN	CN	PMe_2Ph

Figure 1. Geometry and numbering system for icosahedral metallaheteroboranes.

The structures were readily solved by direct methods (MULTAN78 for **2**; SHELXS-86 for **3**; SHELXTL-PC for **5**) and standard Fourier techniques. All hydrogen atoms were visible in difference Fouriers phased on the non-hydrogen atoms, and were included in the final least-squares refinements. Note that some of the hydrogen positions in **2** differ significantly from idealized locations, but are qualitatively correct. The final difference Fouriers were featureless, the largest peak being 0.82 e/Å^3 for **2**, 0.12 e/Å^3 for **3**, and 0.23 e/Å^3 for **5**. Additional information may be obtained from the Molecular Structure Center by reference to Report Nos. 92081 (**2**), 93256 (**3**), and 94181 (**5**).

Results and Discussion

A + $(PMe_2Ph)_2Pd(CN)_2$ Reaction. Treatment of $(PMe_2Ph)_2Pd(B_9H_9As_2)$ (**A**) with $(PMe_2Ph)_2Pd(CN)_2$ in refluxing THF results in the formation of $(PMe_2Ph)(CN)Pd(5\text{-}PMe_2Ph\text{-}B_9H_8\text{-}As_2)$ (**1**) in 26.5% isolated yield. The numbering scheme used for icosahedral metallaheteroboranes is as illustrated in Figure 1. There is now ample precedent for this type of phosphine substitution onto a borane cage.[1,2,11-24] In particular, this reaction is analogous to the reaction of **A** with $(PMe_2Ph)_2PdCl_2$, to produce $(PMe_2Ph)ClPd(5\text{-}PMe_2Ph\text{-}B_9H_8As_2)$.[1] In these reactions, use of a palladium reagent to assist in the cage substitution

Table 1. Fractional Coordinates and Isotropic Thermal Parameters for $5\text{-}CN\text{-}1,1\text{-}(PMe_2Ph)_2\text{-}1,2,3\text{-}PdAs_2B_9H_8$ (**2**)[a]

atom	x	y	z	B_{iso},[b] Å^2
Pd(1)	9354(1)	587(1)	7271.3(3)	9
As(2)	7980(1)	973(1)	6513.6(5)	12
As(3)	7457(1)	138(1)	1479.3(5)	13
B(4)	7902(9)	1878(9)	7151(5)	15
B(5)	8484(8)	1973(8)	6417(5)	12
B(6)	8564(8)	554(8)	6040(5)	13
B(7)	6343(8)	−71(9)	6329(6)	14
B(8)	6430(8)	1366(9)	6750(5)	15
B(9)	7070(8)	2339(8)	6271(5)	12
B(10)	7477(8)	1555(8)	5604(5)	11
B(11)	7073(8)	76(9)	5633(6)	14
B(12)	6206(8)	1195(9)	5797(6)	15
C(13)	9316(8)	2981(7)	6388(4)	15
N(14)	9940(7)	3710(7)	6390(4)	21
P(15)	10206(2)	1071(2)	8480(1)	13
C(16)	9305(9)	1427(10)	9041(5)	38
C(17)	11054(9)	2358(8)	8504(5)	35
C(18)	11116(7)	−2(7)	9056(4)	23
C(19)	12077(7)	311(8)	9618(4)	28
C(20)	12770(8)	−539(8)	10039(5)	32
C(21)	12500(8)	−1712(8)	9894(5)	33
C(22)	11525(8)	−2027(8)	9347(5)	32
C(23)	10826(7)	−1167(7)	8929(5)	27
P(24)	10998(2)	−17(2)	7043(1)	12
C(25)	11487(8)	998(8)	6478(5)	32
C(26)	12291(8)	−300(8)	7782(5)	33
C(27)	10802(7)	−1382(7)	6565(4)	26
C(28)	10849(7)	−1518(8)	5846(4)	28
C(29)	10693(7)	−2616(8)	5526(5)	30
C(30)	10490(7)	−3565(8)	5905(5)	32
C(31)	10422(7)	−3437(7)	6619(5)	30
C(32)	10571(7)	−2350(7)	6937(5)	27
H(1)	801(7)	246(8)	757(5)	32(17)
H(2)	919(6)	30(7)	570(4)	12(13)
H(3)	566(6)	−63(7)	628(4)	3(12)
H(4)	579(7)	165(8)	701(5)	32(16)
H(5)	681(7)	317(8)	617(5)	20(15)
H(6)	745(6)	188(7)	508(4)	9(13)
H(7)	691(6)	−32(7)	522(4)	4(13)
H(8)	546(7)	131(7)	540(5)	22(15)
H(9)	985(8)	166(9)	960(6)	38(18)
H(10)	864(10)	189(11)	879(6)	55(23)
H(11)	878(8)	64(9)	914(5)	35(18)
H(12)	1147(11)	276(12)	906(8)	75(25)
H(13)	1207(11)	222(12)	838(7)	84(28)
H(14)	1044(11)	308(12)	802(7)	71(27)
H(15)	1232(7)	125(8)	978(5)	19(15)
H(16)	1358(8)	−39(8)	1047(5)	26(16)
H(17)	1336(8)	−232(9)	1021(5)	33(18)
H(18)	1085(18)	−295(20)	947(12)	212(45)
H(19)	1004(11)	−158(12)	840(7)	83(27)
H(20)	1230(8)	51(8)	635(5)	32(17)
H(21)	1084(7)	119(7)	597(5)	14(14)
H(22)	1194(16)	187(18)	693(11)	170(39)
H(23)	1224(8)	−104(9)	817(6)	33(18)
H(24)	1302(8)	−67(9)	746(5)	40(19)
H(25)	1263(13)	58(14)	826(9)	111(31)
H(26)	1109(7)	−67(7)	552(5)	23(15)
H(27)	1081(9)	−267(10)	499(6)	54(21)
H(28)	1063(9)	−458(10)	574(6)	56(21)
H(29)	1013(8)	−419(9)	694(5)	29(17)
H(30)	1041(7)	−225(8)	757(5)	30(17)

[a] Fractional coordinates are $\times 10^4$ for non-hydrogen atoms and $\times 10^3$ for hydrogen atoms. B_{iso} values are $\times 10$. [b] Isotropic values for those atoms refined anisotropically are calculated using the formula given by: Hamilton, W. C. *Acta Crystallogr.* **1959**, *12*, 609.

---

(11) Mullica, D. F.; Sappenfield, E. L.; Stone, F. G. A.; Woollam, S. F. *Organometallics* **1994**, 13, 157.

(12) Ferguson, G.; Gallagher, J. F.; McGrath, M.; Sheehan, J. P.; Spalding, T. R.; Kennedy, J. D. *J. Chem. Soc., Dalton Trans.* **1993**, 27.

(13) Ferguson, G.; Gallagher, J. F.; McGrath, M.; Sheehan, J. P.; Spalding, T. R.; Kennedy, J. D. *J. Chem. Soc., Dalton Trans.* **1993**, 35.

(14) Bould, J.; Brint, P.; Kennedy, J. D.; Thornton-Pett, M. *J. Chem. Soc., Dalton Trans.* **1993**, 2335.

(15) Ferguson, G.; Gallagher, J. F.; Sheehan, J. P.; Spalding, T. R.; Kennedy, J. D.; Macias, R. *J. Chem. Soc., Dalton Trans.* **1993**, 3147.

(16) Jones, J. H.; Stibr, B.; Kennedy, J. D.; Thornton-Pett, M. *Coll. Czech. Chem. Commun.* **1993**, 58, 2924.

(17) Bould, J.; Kennedy, J. D.;Thornton-Pett, M. *J. Chem. Soc., Dalton Trans.* **1992**, 563.

(18) McGrath, M.; Spalding, T. R.; Fontaine, X. L. R.; Kennedy, J. D.; Thornton-Pett, M. *J. Chem. Soc., Dalton Trans.* **1991**, 3223.

(19) Fontaine, X. L. R.; Fowkes, H.; Greenwood, N. N.; Kennedy, J. D.; Thornton-Pett, M. *J. Chem. Soc., Dalton Trans.* **1987**, 1431.

(20) Cheek, Y. M.; Kennedy, J. D.; Thornton-Pett, M. *Inorg. Chim. Acta* **1985**, 99, L43.

(21) King III, R. E.; Miller, S. B.; Knobler, C. B.; Hawthorne, M. F. *Inorg. Chem.* **1983**, 22, 3548.

(22) Alcock, N. W.; Taylor, J. G.; Wallbridge, M. G. H. *J. Chem. Soc. Chem. Commun.* **1983**, 1168.

(23) Jung, C. W.; Hawthorne, M. F. *J. Am. Chem. Soc.* **1980**, 102, 3024.

(24) Miller, H. C.; Miller, N. E.; Muetterties, E. L. *Inorg. Chem.* **1964**, 3, 1456.

Table 2. Fractional Coordinates and Isotropic Thermal Parameters for 1-^{t}BuNC-5-CN-1-PMe$_2$Ph-1,2,3-PdAs$_2$B$_9$H$_8$ (**3**)[a]

atom	*x*	*y*	*z*	B_{iso}[b] (Å^2)
Pd(1)	9980.8(3)	7690.3(3)	3613.6(4)	10
As(2)	10393.0(5)	6998.8(4)	6149(1)	13
As(3)	11283.1(5)	5622.9(4)	4550(1)	14
B(4)	12009(5)	6980(5)	3924(6)	15
B(5)	11830(5)	8475(5)	4681(6)	13
B(6)	11093(5)	8593(5)	5952(6)	11
B(7)	12428(5)	6092(5)	6923(6)	16
B(8)	13140(5)	6101(5)	5577(6)	15
B(9)	13311(5)	7544(5)	5410(6)	13
B(10)	12784(5)	8446(5)	6661(6)	12
B(11)	12153(5)	7619(5)	7526(6)	12
B(12)	13530(5)	7019(5)	7182(6)	12
C(13)	8109(5)	7952(4)	3205(5)	14
N(14)	7044(4)	8065(3)	2947(4)	14
C(15)	5658(4)	8203(4)	2562(5)	14
C(16)	5300(6)	7007(5)	2481(7)	22
C(17)	4987(6)	8760(5)	1053(7)	22
C(18)	5403(5)	8964(5)	3776(7)	20
C(19)	8437(5)	9413(4)	611(6)	17
P(20)	9354(1)	7995(1)	1094(1)	12
C(21)	8317(4)	6991(4)	−153(5)	12
C(22)	10548(5)	7956(5)	335(6)	17
C(23)	8145(5)	6024(4)	389(6)	17
C(24)	7374(5)	5261(5)	−578(6)	18
C(25)	6782(5)	5463(4)	−2083(6)	17
C(26)	6954(5)	6421(4)	−2642(5)	17
C(27)	7709(5)	7191(4)	−1684(6)	17
C(28)	11817(4)	9509(4)	3788(5)	13
N(29)	11799(4)	10245(4)	3098(5)	18
H(1)	1223(4)	776(4)	867(16)	19(9)
H(2)	1054(4)	928(3)	621(4)	0(7)
H(3)	1210(5)	678(4)	294(6)	26(9)
H(4)	1378(5)	537(5)	553(6)	27(9)
H(5)	1264(6)	539(5)	762(7)	47(11)
H(6)	1413(5)	764(5)	522(6)	37(10)
H(7)	1327(5)	916(4)	731(5)	21(9)
H(8)	1446(4)	678(4)	807(5)	12(8)
H(9)	440(5)	710(4)	228(5)	8(8)
H(10)	542(5)	649(5)	169(6)	28(10)
H(11)	577(5)	665(5)	345(7)	32(10)
H(12)	521(5)	948(5)	118(6)	25(9)
H(13)	522(5)	831(5)	33(6)	29(10)
H(14)	411(5)	887(4)	71(5)	10(8)
H(15)	580(6)	859(5)	469(7)	44(12)
H(16)	564(5)	967(5)	387(6)	23(9)
H(17)	448(6)	911(4)	349(6)	28(10)
H(18)	897(5)	997(5)	125(6)	23(9)
H(19)	821(5)	952(4)	−46(7)	27(9)
H(20)	775(5)	944(4)	79(5)	13(9)
H(21)	1091(5)	716(5)	38(6)	34(10)
H(22)	1016(4)	826(4)	−59(6)	13(8)
H(23)	1117(6)	845(5)	97(6)	35(10)
H(24)	851(4)	586(4)	127(5)	0(8)
H(25)	731(5)	471(4)	−21(6)	16(9)
H(26)	624(5)	499(4)	−270(5)	16(9)
H(27)	654(6)	660(5)	−367(7)	40(11)
H(28)	779(5)	781(4)	−204(5)	18(9)

[a] Fractional coordinates are ×10^4 for non-hydrogen atoms and ×10^3 for hydrogen atoms. B_{iso} values are ×10. [b] Isotropic values for those atoms refined anisotropically are calculated using the formula given by: Hamilton, W. C. *Acta Crystallogr.* **1959**, *12*, 609.

results in much faster reaction and better yields than without. A possible equation is as indicated in eq 1. A gray solid,

$$(PMe_2Ph)_2Pd(B_9H_9As_2) + (PMe_2Ph)_2Pd(CN)_2 \rightarrow (PMe_2Ph)(CN)Pd(5\text{-}PMe_2Ph\text{-}B_9H_8As_2)\ (\mathbf{1}) + 2PMe_2Ph + Pd^0 + HCN \quad (1)$$

probably elemental Pd, has been observed as a final product of a number of similar palladium-assisted borane cage substitution reactions. In addition, we have shown the reaction of **A** with (PMe$_2$Ph)$_2$PdCl$_2$ gives (PMe$_2$Ph)ClPd(6-Cl-5-PMe$_2$Ph-B$_9$H$_7$-As$_2$). This demonstrates a palladium-assisted cage substitution

Table 3. Fractional Coordinates and Isotropic Thermal Parameters for 4,5-(CN)$_2$-1,1-(PMe$_2$Ph)$_2$-1,2,3-PdC$_2$B$_9$H$_9$ (**5**)[a]

atom	*x*	*y*	*z*	B_{iso}[b] (Å^2)
Pd(1)	4530.9(5)	2160.5(2)	6790.5(4)	11
C(2)	6464(6)	2804(3)	7888(5)	15
C(3)	6846(6)	2277(3)	7145(5)	13
B(4)	6050(7)	2406(4)	5881(5)	11
B(5)	4945(7)	3126(4)	5870(5)	13
B(6)	5159(7)	3305(4)	7221(6)	13
B(7)	7970(7)	2957(4)	7701(6)	17
B(8)	7709(7)	2698(4)	6412(6)	16
B(9)	6539(7)	3277(4)	5647(6)	16
B(10)	5925(7)	3850(4)	6448(6)	15
B(11)	6830(7)	3648(4)	7719(6)	15
B(12)	7676(7)	3610(4)	6755(6)	19
C(13)	5981(6)	1788(4)	5128(5)	16
N(14)	5946(5)	1315(3)	4587(4)	23
C(15)	3710(6)	3329(3)	5003(5)	13
N(16)	2808(6)	3483(3)	4352(4)	21
F(17)	4452(2)	936(1)	6851(1)	14
C(18)	6110(7)	536(4)	7100(6)	18
C(19)	3566(8)	494(4)	5697(6)	20
C(20)	3835(6)	595(3)	7871(5)	16
C(21)	2800(6)	115(3)	7745(6)	20
C(22)	2346(7)	−91(4)	8574(6)	24
C(23)	2914(7)	171(4)	9506(6)	24
C(24)	3966(7)	640(4)	9651(6)	23
C(25)	4418(7)	851(4)	8846(5)	20
P(26)	2503(2)	2336(1)	7085(1)	15
C(27)	1623(7)	3108(4)	6475(7)	22
C(28)	2655(8)	2497(5)	8406(6)	23
C(29)	1221(6)	1667(3)	6687(5)	14
C(30)	774(6)	1505(4)	5653(5)	20
C(31)	−240(7)	1018(4)	5304(6)	26
C(32)	−811(7)	697(4)	5987(6)	27
C(33)	−389(7)	841(4)	6995(6)	22
C(34)	624(6)	1332(4)	7352(6)	18
H(1)	643(5)	262(3)	853(4)	15(10)
H(2)	716(5)	185(3)	739(4)	0(8)
H(3)	451(5)	355(3)	764(4)	5(8)
H(4)	885(6)	285(3)	825(4)	27(10)
H(5)	841(6)	245(3)	622(4)	23(10)
H(6)	568(5)	345(3)	493(4)	6(8)
H(7)	562(6)	440(3)	621(4)	26(10)
H(8)	707(5)	402(3)	836(4)	12(9)
H(9)	849(6)	394(3)	677(4)	23(10)
H(10)	595(6)	12(3)	708(4)	14(11)
H(11)	646(6)	68(3)	661(5)	27(12)
H(12)	660(7)	67(4)	773(6)	47(15)
H(13)	281(6)	57(3)	560(4)	3(10)
H(14)	398(7)	71(4)	521(6)	49(15)
H(15)	370(7)	−1(4)	575(5)	38(13)
H(16)	241(5)	−8(3)	713(4)	10(10)
H(17)	166(6)	−37(3)	845(4)	18(11)
H(18)	269(5)	5(3)	1008(4)	8(9)
H(19)	448(6)	80(3)	1034(5)	24(11)
H(20)	509(5)	117(3)	892(4)	2(9)
H(21)	211(6)	350(3)	677(4)	20(11)
H(22)	138(6)	306(3)	571(5)	30(12)
H(23)	81(7)	312(3)	661(5)	30(12)
H(24)	303(5)	215(3)	873(4)	1(9)
H(25)	335(7)	288(4)	864(5)	39(12)
H(26)	178(8)	261(4)	844(5)	52(15)
H(27)	117(6)	170(3)	524(5)	19(11)
H(28)	−49(6)	94(3)	469(5)	18(11)
H(29)	138(6)	41(3)	579(5)	22(12)
H(30)	−73(7)	68(4)	743(5)	40(15)
H(31)	94(6)	143(3)	799(5)	22(12)

[a] Fractional coordinates are ×10^4 for non-hydrogen atoms and ×10^3 for hydrogen atoms. B_{iso} values are ×10. [b] Isotropic values for those atoms refined anisotropically are calculated using the formula given by: Hamilton, W. C. *Acta Crystallogr.* **1959**, *12*, 609.

Table 4. ^{11}B NMR Data

cmpd	chem shift (ppm), rel intens, $J_{\mathrm{B-H}}$ (Hz)
1[a]	8.6, 1B, d, $J_{\mathrm{B-P}}$ 132 Hz; 1.6, 1B, d; 0.8, 2B, d; −0.9, 2B, d; −9.5, 1B, d; −10.9, 2B, d
2[b]	11.5, 1B, s; 3.2, 4B, d; −1.2, 1B, d; −7.6, 2B, d, 137; −13.2, 1B, d, 123
3[a]	7.5, 1B, s; 3.7, 4B, d; 1.1, 1B, d, 146; −9.1, 2B, d, 147; −11.1, 1B, d
4[c]	5.6, 1B, d, 117; −9.5, 3B, d; −16.1, 4B, br d; −21.2, 1B, d, 130
5[d]	−1.6, 1B, d, 143; −6.2, 1B, s; −12.1, 1B, d; −13.5, 1B, d; −16.9, 1B, d; −18.4, 1B, d; −19.0, 1B, d; −20.4, 1B, d; −21.9, 1B, s

[a] CH_2Cl_2 solvent. [b] CH_2Cl_2/CH_3CN solvents. [c] $CDCl_3$ solvent. [d] CD_3CN solvent.

of a chloro group. A similar palladium-assisted cage substitution of a cyano group has not been observed thus far.

The ^{11}B NMR spectra of **1** and its chloro analogue, $(PMe_2Ph)ClPd(5\text{-}PMe_2Ph\text{-}B_9H_8As_2)$, are nearly identical, as expected. The greatest difference is the position of the phosphorus-coupled doublet signal, which is at 8.6 ppm for **1** (see Table 4), and 13.2 ppm for the chloro analogue. The B−P coupling constants are 132 and 137 Hz, respectively, which is within the range of observed values for phosphines bonded to cage boranes.[1,2,11−24] The C_s symmetrical $5\text{-}PMe_2Ph\text{-}1,2,3\text{-}PdAs_2B_9H_8$ fragment is expected to exhibit a 2:2:2:1:1:1 peak area ratio pattern. Due to near peak overlap, the area ratio assignments (see Table 4) are somewhat uncertain for the signals at +1.6 and −0.9 ppm. One is area 1 and the other is area 2; however, both appear as shoulders on the peak at 0.8 ppm.

The $^{31}P\{^1H\}$ and ^{1}H NMR spectra of **1** and its chloro analogue are similar. Both exhibit a singlet (Pd−*P*) and a 1:1:1:1 quartet (B−*P*) in their $^{31}P\{^1H\}$ NMR spectra, and two methyl doublet (P*Me*$_2$Ph) environments are observed in each ^{1}H NMR spectrum. There are only two signals observed for four methyl groups because each phosphine can be aligned, with rotation about the P−B or P−Pd bond, such that the two methyl groups straddle the mirror plane of the molecule.

A + ^{t}BuNC Reactions. Reaction of **A** with varying stoichiometries of ^{t}BuNC in refluxing THF also results in cage substitution reactions. The first product isolated was $(PMe_2Ph)_2Pd(5\text{-}CN\text{-}B_9H_8As_2)$ (**2**), see eq 2. At the outset, this seems to contradict our earlier statement that a palladium reagent is required to effect such a B−H bond activation, with subsequent substitution of a ligand onto boron. However, because of the necessity of long reflux times, it is plausible that a phosphine dissociates from **A**, to be replaced by ^{t}BuNC. This species then activates a B−H bond on another molecule of **A**, to give the observed products.

Three reactions were attempted, varying the stoichiometry of **A**:^{t}BuNC and the heating time. The first reaction used a 1:2 ratio of **A**:^{t}BuNC and 15 h of THF reflux. It resulted in the formation of $(PMe_2Ph)_2Pd(5\text{-}CN\text{-}B_9H_8As_2)$ (**2**), as the only identifiable boron-containing product (other than the starting material). Dealkylation of the isocyanide is a known process,

$$(PMe_2Ph)_2Pd(B_9H_9As_2) + {}^tBuNC \rightarrow (PMe_2Ph)_2Pd(5\text{-}CN\text{-}B_9H_8As_2)\ (\mathbf{2}) + [Me_3CH \text{ or } Me_2C{=}CH_2] \quad (2)$$

for instance, heating $(Cp^*)_2V$ and ^{t}BuNC together in refluxing hexane yields $Cp^*V(CN)(^tBuNC)$.[25] Refluxing $[Mo(^tBuNC)_7][PF_6]$ in ethanol yields $[Mo(^tBuNC)_6(CN)][PF_6]$.[26] The mechanism may be radical in nature, or ionic, by producing the tertiary Me_3C^+ ion, on the way to isobutane or isobutylene.

Table 5. $^{31}P\{^1H\}$ NMR Data

cmpd	chem shift (ppm), multiplicity, $J_{\mathrm{B-P}}$ (Hz)
1[a]	−5.1, singlet; −4.3, 1:1:1:1 quartet, 130
2[a]	−6.9, singlet
3[a]	−1.2, singlet
4[a]	−2.4, singlet
5[b]	1.6, singlet

[a] $CDCl_3$ solvent. [b] CD_3CN solvent.

Table 6. ^{1}H NMR Data

cmpd	chem shift (ppm), rel intens, assignt, multiplicity, $J_{\mathrm{H-P}}$ (Hz)
1[a]	1.712, 6H, P*Me*$_2$, d, 10.6; 1.894, 6H, P*Me*$_2$, d, 12.0; 7.4−7.8, 10H, P*Ph*, mult
2[a]	1.678, 12H, P*Me*$_2$, filled-in d, 9.4; 7.43−7.48, 10H, P*Ph*, multiplets
3[a]	1.308, 9H, ^{t}*BuNC*, s; 2.026, 6H, P*Me*$_2$, d, 10.8; 7.5−7.9, 5H, P*Ph*, multiplets
4[a]	1.526, 12H, P*Me*$_2$, filled-in d, 9.5; 2.639, 2H, *H*-carborane, br; 7.35−7.47, 10H, P*Ph*, mult
5[b]	1.594, 6H, P*Me*$_2$, filled-in d, 11.3; 1.732, 6H, P*Me*$_2$, filled-in d, 10.9; 2.66, 1H, *H*-carborane, br; 3.38, 1H, *H*-carborane, br; 7.48−7.54, 10H, P*Ph*, mult

[a] $CDCl_3$ solvent. [b] CD_3CN solvent.

The second reaction used a 1:33 ratio of **A**:^{t}BuNC. It produced a mixture of **2** and $(^tBuNC)(PMe_2Ph)Pd(5\text{-}CN\text{-}B_9H_8As_2)$ (**3**), in approximately 3:7 ratio, after refluxing in THF for 4 days. The latter compound **3** is derived from **2** simply by substitution of PMe_2Ph with ^{t}BuNC. Thus, the higher the concentration of ^{t}BuNC in solution, the more one expects to observe that **3** is formed in preference to **2**. A kind of equilibrium such as eq 3 may be operative.

$$(PMe_2Ph)_2Pd(5\text{-}CN\text{-}B_9H_8As_2)\ (\mathbf{2}) + {}^tBuNC \rightleftharpoons ({}^tBuNC)(PMe_2Ph)Pd(5\text{-}CN\text{-}B_9H_8As_2)\ (\mathbf{3}) + PMe_2Ph \quad (3)$$

Equation 3 is supported by the result of the third reaction, which used a 1:30 ratio of **A**:^{t}BuNC, and in which no **2** was formed; only **3** and **1** were observed after refluxing in THF 7 days. Of the products isolated from this reaction, 35.2% was unreacted **A**; a 3.00% yield of **3**, and a 6.6% yield of **1** were obtained. These results are essentially the same as for the second reaction, except that in this more carefully done (to establish yields) experiment, **1** was also observed as a product. In fact, **1** may have been present in the second reaction, and went undetected.

Clearly, then, at least two different processes occur in this reaction: one substitutes a phosphine onto the B(5) position; the other substitutes a cyanide at this position, possibly via a palladium-assisted process resulting in eq 4. Although this

$$(\text{cage}){-}H + {}^tBuNC \rightarrow (\text{cage}){-}CN + [Me_3CH \text{ or } Me_2C{=}CH_2] \quad (4)$$

reaction produces both **3** and **1**, it is not the most efficient means to do so. Use of a palladium reagent to effect the substitutions results in higher yields; see eqs 1 and 5.

---

(25) Gambarotta, S.; Floriani, C.; Chiesi-Villa, A.; Guastini, C. *Inorg. Chem.* **1984**, 23, 1739.

(26) Giandomenico, C. M.; Hanau, L. H.; Lippard, S. J. *Organometallics* **1982**, 1, 142.

Table 7. Infrared Data[a]

cmpd	ν_{max} (in cm^{-1})
1	3056 (2), 2519 (vs), 2116 (m), 1435 (s), 1416 (m), 1298 (w), 1285 (m), 1115 (m), 1018 (m), 984 (w), 961 (m), 949 (m), 910 (vs), 860 (m), 845 (w), 743 (s), 725 (m), 716 (w), 691 (s), 484 (m), 421 (m)
2	3440 (w, br), 2969 (w), 2909 (w), 2558 (s), 2529 (vs), 2188 (w), 1572 (w), 1480 (w), 1435 (s), 1416 (m), 1312 (w), 1285 (w), 1262 (w), 1105 (m), 1026 (w, br), 990 (m), 945 (s), 905 (vs), 831 (w), 802 (m, br), 760 (m), 747 (m), 714 (m), 696 (m), 490 (m), 432 (w), 419 (w)
3	3052 (w), 2984 (m), 2552 (vs), 2529 (vs), 2199 (vs), 1487 (w), 1474 (w), 1458 (w), 1435 (s), 1422 (m), 1400 (m), 1385 (w), 1372 (m), 1298 (w), 1287 (m), 1231 (w), 1190 (m), 1105 (m), 1073 (w), 982 (m), 957 (s), 922 (vs), 860 (w), 847 (m), 779 (w), 741 (m), 718 (m), 693 (m), 523 (w), 480 (w), 432 (m)
4	3434 (w), 3075 (w), 3052 (w), 3040 (w), 2579 (s), 2531 (s), 1485 (w), 1435 (s), 1416 (m), 1406 (m), 1385 (m), 1310 (w), 1283 (w), 1101 (m), 1071 (w), 1026 (m), 999 (w), 976 (w), 945 (s), 905 (s), 870 (w), 839 (w), 746 (s), 735 (s), 714 (m), 694 (s), 683 (m), 484 (m), 446 (m), 424 (m)
5	3432 (w), 3069 (w), 3061 (w), 3005 (w), 2975 (w), 2625 (w), 2560 (s), 2531 (s), 2195 (m), 1489 (w), 1437 (s), 1418 (m), 1402 (w), 1300 (m), 1287 (m), 1107 (m), 1007 (w), 972 (w), 949 (s), 928 (s), 910 (s), 841 (m), 743 (s), 714 (m), 692 (s), 683 (m), 509 (w), 486 (m), 440 (m)

[a] KBr wafer.

A + (^{t}BuNC)$_2$PdCl$_2$. Reaction of **A** with 1.0 equiv of (^{t}BuNC)$_2$PdCl$_2$ in refluxing THF for 3 days results in formation of **3** in 28.3% yield, with no observed **2**, eq 5. Only a small

$$(PMe_2Ph)_2Pd(B_9H_9As_2) + (^tBuNC)_2PdCl_2 \rightarrow (^tBuNC)(PMe_2Ph)Pd(5\text{-}CN\text{-}B_9H_8As_2)\ (\mathbf{3}) + PMe_2Ph + [Me_3CH \text{ or } Me_2C{=}CH_2] + PdCl_2 \quad (5)$$

amount of **A** was recovered unreacted, in contrast to the reactions with ^{t}BuNC alone. Therefore, this method is currently the choice route to compound **3**. Note that the non-boron products in eq 5 are speculative at this time. Other possibilities might include Pd^0, HCl, etc.

Spectroscopy of 2 and 3. Comparison of the ^{11}B NMR spectra of **2** and **3** (see Table 4) shows that they are nearly the same. There is some 1−2 ppm shifting of the peak positions, but the most diagnostic is the location of the B(5) singlet, at 11.5 ppm for **2** and 7.5 ppm for **3**. Comparison of these spectra to that of **A**[1,18] shows only that they occupy the same region of the spectrum; many signals have crossed over others.

The ^{1}H NMR of both **A** and **2**, and indeed all (PMe$_2$Ph)$_2$Pd species where ∠P−Pd−P > 90°, exhibit second order spectra for the P*Me$_2$*Ph methyl protons. The multiplet may be described as a doublet with a broad singlet overlapping it, or a filled-in doublet. This has been speculatively ascribed to partial virtual coupling of the two P nuclei.[1,27] The P−Pd−P angle in **2** is 95.30° (see Table 9), so one expects to observe this phenomenon.

The IR spectra of **2** and **3** both contain two principal B−H stretches near 2500 cm^{-1} (see Table 7), and one C−N stretch near 2200 cm^{-1}. Since **3** contains a B−C−N moiety and a Pd−C−NR moiety, one expects perhaps two observable C−N stretches. It is unclear why this is not the case.

X-ray Structures of 2 and 3. Comparison of the structures of (PMe$_2$Ph)$_2$Pd(B$_9$H$_9$As$_2$) (**A**), (PMe$_2$Ph)$_2$Pd(5-CN-B$_9$H$_8$As$_2$) (**2**), and (^{t}BuNC)(PMe$_2$Ph)Pd(5-CN-B$_9$H$_8$As$_2$) (**3**) (see Figures 2 and 3) shows that they have much in common. In fact, comparison of the unit cell parameters indicates that **A** and **2** appear to be nearly isomorphous. All three have a 12-vertex cage that is significantly distorted from icosahedral symmetry due to the relatively large Pd and As atoms. All of the As−As distances are in the range 2.49−2.54 Å (see Tables 8 and 10), much greater than the typical 1.61 Å C−C distance in a B$_9$H$_9$(CH)$_2$M cage.[28] Since these cages are isoelectronic, the cage distortion is primarily a steric effect, and not an electronic one.

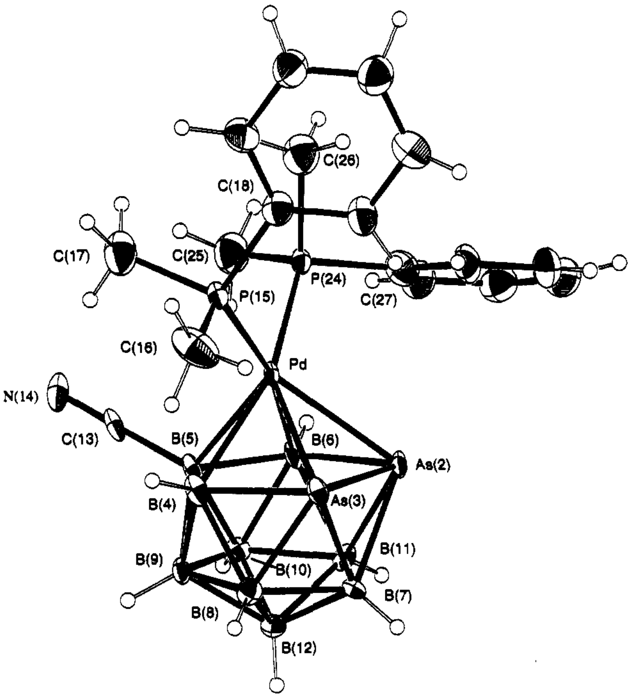

Figure 2. ORTEP diagram of 5-CN-1,1-(PMe$_2$Ph)$_2$-*closo*-PdAs$_2$B$_9$H$_8$ (**2**).

The inclusion of three large heteroatoms in a single triangular face of an icosahedron causes the cage to "flex" outward to accommodate the larger atoms. The effect is illustrated by contrasting intraboron distances between boron atoms adjacent to a heteroatom and boron atoms not adjacent to a heteroatom. Table 12 compares the average B−B distance in the chair-shaped trace defined by atoms 4−5−6−11−7−8 (see Figure 4) to the average B−B distance in the triangle opposite the three heteroatoms, atoms 9−10−12. The average distances in the chair-shaped trace are all longer than those in the triangle, which agree well with the value for B$_{12}$H$_{12}$2−, 1.77 Å.[29]

Comparison of the average distances from B(5) to its five nearest neighbors shows that there is no statistically significant difference between **A**, **2**, and **3**. This implies that cyano substitution for hydride at B(5) results in no significant molecular structural change.

---

(27) Wilkes, L. M.; Nelson, J. H.; McCusker, L. B.; Seff, K.; Mathey, F. *Inorg. Chem.* **1983**, 22, 2476.

(28) Fontaine, X. L. R.; Greenwood, N. N.; Kennedy, J. D.; Nestor, K.; Thornton-Pett, M. *J. Chem. Soc., Dalton Trans.* **1990**, 681.

(29) Lipscomb, W. N. *Boron Hydrides*; W. A. Benjamin, Inc.: New York, 1963; p 18.

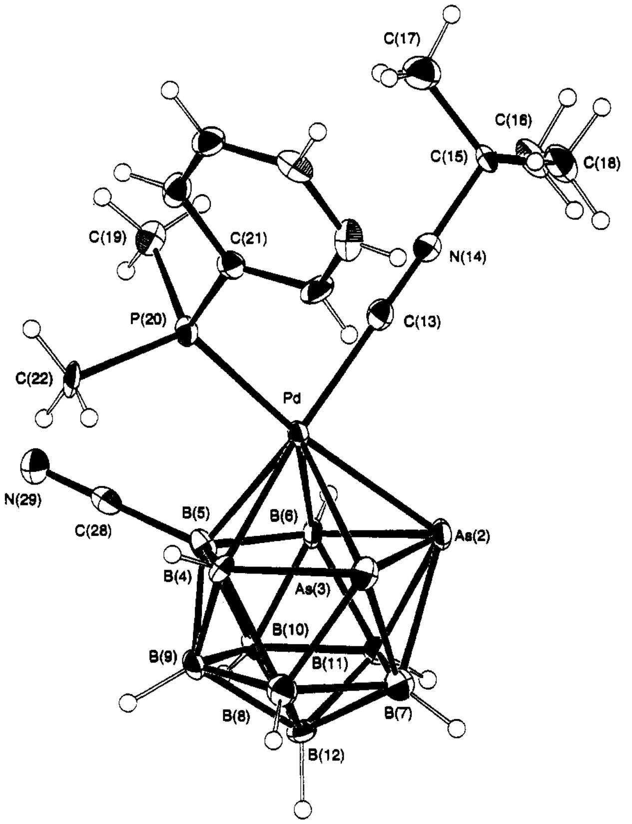

Figure 3. ORTEP diagram of 1-^{t}BuNC-5-CN-1-PMe$_2$Ph-*closo*-1,2,3-PdAs$_2$B$_9$H$_8$ (**3**).

Table 8. Selected Bond Distances (Å) for 5-CN-1,1-(PMe$_2$Ph)$_2$-1,2,3-PdAs$_2$B$_9$H$_8$ (**2**)

(i) Distances to the Pd			
Pd(1)–As(2)	2.6116(10)	Pd(1)–B(4)	2.306(10)
Pd(1)–As(3)	2.5641(6)	Pd(1)–B(5)	2.317(9)
Pd(1)–P(15)	2.3068(22)	Pd(1)–B(6)	2.266(9)
Pd(1)–P(24)	2.3258(21)		
(ii) Distances to As			
As(2)–As(3)	2.4911(13)	As(3)–B(4)	2.228(10)
As(2)–B(6)	2.207(9)	As(3)–B(7)	2.237(10)
As(2)–B(7)	2.225(9)	As(3)–B(8)	2.132(10)
As(2)–B(11)	2.110(10)		
(iii) Interboron Distances			
B(4)–B(5)	1.766(13)	B(7)–B(11)	1.829(14)
B(4)–B(8)	1.862(14)	B(7)–B(12)	1.763(14)
B(4)–B(9)	1.775(13)	B(8)–B(8)	1.782(13)
B(5)–B(6)	1.809(12)	B(8)–B(12)	1.770(14)
B(5)–B(9)	1.752(14)	B(9)–B(10)	1.758(13)
B(5)–B(10)	1.750(13)	B(9)–B(12)	1.777(13)
B(6)–B(10)	1.790(13)	B(10)–B(11)	1.791(14)
B(6)–B(11)	1.871(13)	B(10)–B(12)	1.779(13)
B(7)–B(8)	1.838(14)	B(11)–B(12)	1.773(14)
(iv) Other Distances			
N(14)–C(13)	1.145(11)	C(13)–B(5)	1.575(14)

An attempt to synthesize (^{t}BuNC)$_2$Pd(B$_9$H$_9$As$_2$), by reacting [7,8-As$_2$B$_9$H$_9$]$^{2-}$ with (^{t}BuNC)$_2$PdCl$_2$, eq 6, was made.

$$[\mathrm{Li}]_2[\mathrm{B_9H_9As_2}] + (^t\mathrm{BuNC})_2\mathrm{PdCl_2} \rightarrow (^t\mathrm{BuNC})_2\mathrm{Pd}(\mathrm{B_9H_9As_2}) + 2\mathrm{LiCl} \qquad (6)$$

Table 9. Selected Bond Angles (deg) for 5-CN-1,1-(PMe$_2$Ph)$_2$-1,2,3-PdAs$_2$B$_9$H$_8$ (**2**)

As(2)–Pd(1)–As(3)	57.53(3)	B(5)–Pd(1)–B(6)	46.5(3)
As(2)–Pd(1)–B(6)	53.25(25)	P(15)–Pd(1)–P(24)	95.30(8)
As(3)–Pd(1)–B(4)	54.15(25)	N(14)–C(13)–B(5)	177.9(9)
B(4)–Pd(1)–B(5)	44.9(3)		
Pd(1)–As(2)–As(3)	60.275(21)	Pd(1)–As(3)–As(2)	62.19(3)
Pd(1)–As(2)–B(6)	55.32(25)	Pd(1)–As(3)–B(4)	57.00(26)
As(3)–As(2)–B(7)	56.29(27)	As(2)–As(3)–B(7)	55.83(25)
B(6)–As(2)–B(11)	51.3(4)	B(4)–As(3)–B(8)	50.5(4)
B(7)–As(2)–B(11)	49.8(4)	B(7)–As(3)–B(8)	49.7(4)
As(3)–As(2)–B(6)	94.62(25)	B(8)–B(7)–B(11)	104.9(7)
As(2)–As(3)–B(4)	96.73(25)	B(7)–B(8)–B(9)	109.0(7)
As(3)–B(4)–B(5)	118.4(6)	B(8)–B(9)–B(10)	108.4(7)
B(4)–B(5)–B(6)	110.1(7)	B(9)–B(10)–B(11)	109.1(7)
As(2)–B(6)–B(5)	120.1(6)	B(7)–B(11)–B(10)	108.5(7)

Table 10. Selected Bond Distances (Å) for 1-^{t}BuNC-5-CN-1-PMe$_2$Ph-1,2,3-PdAs$_2$B$_9$H$_8$ (**3**)

(i) Distances to the Pd			
Pd(1)–As(2)	2.5143(9)	Pd(1)–B(4)	2.258(6)
Pd(1)–As(3)	2.6626(10)	Pd(1)–B(5)	2.276(5)
Pd(1)–P(20)	2.3096(14)	Pd(1)–B(6)	2.368(5)
Pd(1)–C(13)	2.008(5)		
(ii) Distances to As			
As(2)–As(3)	2.5410(9)	As(3)–B(4)	2.174(5)
As(2)–B(6)	2.227(5)	As(3)–B(7)	2.218(6)
As(2)–B(7)	2.255(6)	As(3)–B(8)	2.113(6)
As(2)–B(11)	2.134(5)		
(iii) Interboron Distances			
B(4)–B(5)	1.863(8)	B(7)–B(11)	1.862(8)
B(4)–B(8)	1.871(8)	B(7)–B(12)	1.747(8)
B(4)–B(9)	1.781(8)	B(8)–B(9)	1.780(8)
B(5)–B(6)	1.764(7)	B(8)–B(12)	1.765(7)
B(5)–B(9)	1.773(8)	B(9)–B(10)	1.780(7)
B(5)–B(10)	1.789(7)	B(9)–B(12)	1.801(7)
B(6)–B(10)	1.768(7)	B(10)–B(11)	1.767(7)
B(6)–B(11)	1.867(7)	B(10)–B(12)	1.773(7)
B(7)–B(8)	1.824(8)	B(11)–B(12)	1.871(7)
(iv) Other Distances			
N(14)–C(13)	1.138(6)	N(29)–C(28)	1.142(6)
N(14)–C(15)	1.472(6)	C(28)–B(5)	1.563(7)

Table 11. Selected Bond Angles (deg) for 1-^{t}BuNC-5-CN-1-PMe$_2$Ph-1,2,3-PdAs$_2$B$_9$H$_8$ (**3**)

As(2)–Bd(1)–As(3)	58.707(22)	B(4)–Pd(1)–B(5)	48.53(19)
As(2)–Pd(1)–B(6)	54.19(13)	B(5)–Pd(1)–B(6)	44.60(17)
As(3)–Pd(1)–B(4)	51.64(14)		
P(20)–Pd(1)–C(13)	87.05(13)	Pd(1)–C(13)–N(14)	177.6(4)
C(13)–N(14)–C(15)	178.2(4)	N(29)–C(28)–B(5)	178.0(5)
Pd(1)–As(2)–As(3)	63.564(26)	Pd(1)–As(3)–As(2)	57.729(24)
Pd(1)–As(2)–B(6)	59.55(14)	Pd(1)–As(3)–B(4)	54.53(15)
As(3)–As(2)–B(7)	54.69(14)	As(2)–As(3)–B(7)	56.07(15)
B(6)–As(2)–B(11)	50.63(19)	B(4)–As(3)–B(8)	51.73(21)
B(7)–As(2)–B(11)	50.13(20)	B(7)–As(3)–B(8)	49.76(20)
As(3)–As(2)–B(6)	99.78(14)	B(8)–B(7)–B(11)	105.8(4)
As(2)–As(3)–B(4)	92.31(16)	B(7)–B(8)–B(9)	108.2(4)
As(3)–B(4)–B(5)	120.8(3)	B(8)–B(9)–B(10)	109.0(4)
B(4)–B(5)–B(6)	112.2(4)	B(9)–B(10)–B(11)	109.1(4)
As(2)–B(6)–B(5)	114.5(3)	B(7)–B(11)–B(10)	107.6(4)

It appeared to be a successful synthesis, because a purple compound (of the same color as **A**) was chromatographically isolated from the reaction mixture. This purple compound had a ^{11}B NMR spectrum consisting of B–H coupled doublets at δ 10.5, 4.6, −7.2, and −12.5, in peak area ratios 3:3:1:2. This spectrum is nearly identical to that of **A**.[1] However, the compound appeared to be thermally unstable at room temperature, as it decomposed to an unidentified brown substance(s), and was gone within approximately 6 days. We think it possible that the decomposed products may be cyano-substituted products, but no further characterization was attempted. Thermal instability was likewise observed for the analogous 1,1-(^{t}BuNC)$_2$-2,4-Me$_2$-*closo*-1,2,4-PdC$_2$B$_9$H$_9$.[4,30]

Table 12. Triheteroatom Flex Data

cmpd	4-5-6-11-7-8 trace av (Å)	9-10-12 trace av (Å)
A	1.845(16)	1.765(16)
2	1.829(13)	1.771(13)
3	1.842(8)	1.785(7)
5	1.789(10)	1.785(10)
$(PR_3)_2Pt(B_9C_2H_{11})$[40]	1.799(12)	1.767(12)
$Ni(B_9C_2H_{11})_2$[42]	1.800(3)	1.777(3)

Table 13. Selected Bond Distances (Å) for $4,5\text{-(CN)}_2\text{-}1,1\text{-(PMe}_2\text{Ph)}_2\text{-}1,2,3\text{-PdC}_2B_9H_9$ (**5**)

	(i) Distances to the Pd		
Pd(1)−C(2)	2.482(6)	Pd(1)−B(4)	2.300(7)
Pd(1)−C(3)	2.332(6)	Pd(1)−B(5)	2.319(7)
Pd(1)−P(17)	2.3151(16)	Pd(1)−B(6)	2.288(7)
Pd(1)−P(26)	2.2703(16)		
	(ii) Distances to Carborane C		
C(2)−C(3)	1.548(8)	C(3)−B(4)	1.724(9)
C(2)−B(6)	1.704(9)	C(3)−B(7)	1.766(9)
C(2)−B(7)	1.676(9)	C(3)−B(8)	1.708(9)
C(2)−B(11)	1.668(9)		
	(iii) Interboron Distances		
B(4)−B(5)	1.777(10)	B(7)−B(12)	1.754(11)
B(4)−B(8)	1.770(9)	B(8)−B(9)	1.758(10)
B(4)−B(9)	1.776(10)	B(8)−B(12)	1.787(11)
B(5)−B(6)	1.833(10)	B(9)−B(10)	1.774(10)
B(5)−B(9)	1.785(10)	B(9)−B(12)	1.770(10)
B(5)−B(10)	1.760(10)	B(10)−B(11)	1.784(11)
B(6)−B(11)	1.807(9)	B(10)−B(12)	1.811(10)
B(7)−B(8)	1.781(11)	B(11)−B(12)	1.770(10)
B(7)−B(11)	1.766(10)		
	(iv) Other Distances		
N(14)−C(13)	1.154(8)	C(13)−B(4)	1.544(10)
N(16)−C(15)	1.145(7)	C(15)−B(5)	1.546(10)

Table 14. Selected Bond Angles (deg) for $4,5\text{-(CN)}_2\text{-}1,1\text{-(PMe}_2\text{Ph)}_2\text{-}1,2,3\text{-PdC}_2B_9H_9$ (**5**)

C(2)−Pd(1)−C(3)	37.36(20)	B(5)−Pd(1)−B(6)	46.89(25)
C(2)−Pd(1)−B(6)	41.62(22)	P(17)−Pd(1)−P(26)	95.52(6)
C(3)−Pd(1)−B(4)	43.69(23)	N(14)−C(13)−B(4)	178.1(7)
B(4)−Pd(1)−B(5)	45.24(24)	N(16)−C(15)−B(5)	178.9(6)
Pd(1)−C(2)−C(3)	66.1(3)	Pd(1)−C(3)−C(2)	76.6(3)
Pd(1)−C(2)−B(6)	63.1(3)	Pd(1)−C(3)−B(4)	67.2(3)
C(3)−C(2)−B(7)	66.3(4)	C(2)−C(3)−B(7)	60.3(4)
B(6)−C(2)−B(11)	64.8(4)	B(4)−C(3)−B(8)	62.1(4)
B(7)−C(2)−B(11)	63.8(4)	B(7)−C(3)−B(8)	61.6(4)
C(3)−C(2)−B(6)	108.1(5)	C(3)−B(4)−B(5)	104.6(5)
C(2)−C(3)−B(4)	115.5(5)	B(4)−B(5)−B(6)	103.2(5)
C(2)−B(6)−B(5)	107.7(5)	B(8)−B(9)−B(10)	108.4(5)
B(8)−B(7)−B(11)	106.9(5)	B(9)−B(10)−B(11)	106.8(5)
B(7)−B(8)−B(9)	108.6(5)	B(7)−B(11)−B(10)	109.0(5)

Palladacarboranes. The palladacarborane $(PMe_2Ph)_2Pd(B_9C_2H_{11})$ (**4**) was synthesized by conventional means from $[Me_3NH][B_9C_2H_{12}]$ and $(PMe_2Ph)_2PdCl_2$; see eqs 7 and 8.

$$[Me_3NH][B_9C_2H_{12}] + 2BuLi \rightarrow Li_2[B_9C_2H_{11}] + 2BuH + Me_3N \quad (7)$$

$$Li_2[B_9C_2H_{11}] + (PMe_2Ph)_2PdCl_2 \rightarrow (PMe_2Ph)_2Pd(B_9C_2H_{11})\ (\mathbf{4}) + 2LiCl \quad (8)$$

Compound **4** is isoelectronic with **A** and is a new compound; however, since several analogues have been made, it was not fully characterized, and discussion of **4** will be limited. The NMR spectra of **4** are consistent with its expected icosahedral structure with C_s symmetry, including a filled-in doublet for the $(P\mathit{Me}_2Ph)_2Pd$ methyl signal in the ^1H NMR.

4 + $(^tBuNC)_2PdCl_2$. For comparison to reactions with **A**, a reaction of **4** with 1.0 equiv of $(^tBuNC)_2PdCl_2$ in refluxing THF for 8 h was attempted. The analogous arsaborane reaction forms $(^tBuNC)(PMe_2Ph)Pd(5\text{-CN-}B_9H_8As_2)$ (**3**), but the carborane reaction results in several identifiable products, none of which is the carborane analogue of **3** and only one of which is fully characterized here. Two of these products are 9- and 10-PMe_2Ph-*nido*-7,8-$C_2B_9H_{11}$, which are tentatively assigned (via ^{11}B NMR spectra) by comparison to the known (PPh_3−) analogues.[10] Another product is tentatively assigned the formulation 4-CN-1,1-$(PMe_2Ph)_2$-*closo*-1,2,3-$PdC_2B_9H_{10}$, based upon NMR evidence. We intend that these products shall be fully characterized in a future publication. Observation of the PMe_2Ph-*nido*-7,8-$C_2B_9H_{11}$ products may indicate that the starting material **4** is degrading in solution, by losing palladium from the cage.

The product fully characterized from this reaction was determined to be $(PMe_2Ph)_2Pd(4,5\text{-(CN)}_2\text{-}B_9C_2H_9)$ (**5**), eq 9. This, then, is the first example of a dicyano-substituted metallacarborane, so far as we are aware.

$$(PMe_2Ph)_2Pd(B_9C_2H_{11}) + (^tBuNC)_2PdCl_2 \rightarrow (PMe_2Ph)_2Pd(4,5\text{-(CN)}_2\text{-}B_9C_2H_9)\ (\mathbf{5}) + 2[Me_3CH \text{ or } Me_2C{=}CH_2] + PdCl_2 \quad (9)$$

NMR Studies of 5. Compound **5** has a distinctive ^{11}B NMR spectrum that requires all nine boron atoms to be chemically inequivalent. The molecule thus has C_1 symmetry. Two of the nine signals are singlets, indicating where the cyano groups are substituted onto the cage. The $^{31}P\{^1H\}$ and ^1H NMR spectra are inconsistent with the C_1 symmetry of the molecule, as determined by X-ray diffraction (see Figure 5). Since there is no mirror plane to relate the two phosphorus nuclei, they should be inequivalent, however only a singlet is observed in the room temperature $^{31}P\{^1H\}$ NMR spectrum.

Thus, to determine the nature of this phenomenon, a variable temperature $^{31}P\{^1H\}$ NMR study was undertaken. At 21 °C only one sharp singlet is observed at δ −0.9 ppm. This signal coalesces between −50 and −55 °C, to be replaced with two doublets at δ 7.1 and −6.4 ppm ($^2J_{P-P}$ = 44 Hz), in the −90 °C spectrum.

These results cannot be due merely to rapid rotation of the $[(PMe_2Ph)_2Pd]$ moiety with respect to the pentagonal bonding face of the carborane cage at higher temperatures, in a propeller-like fashion (which is very commonly observed, *vide infra*). This is because there is no symmetric intermediate through which two or more fluxional rotamers can exchange.

The coalescence temperature T_c for the (intermolecular) exchange of the two phosphorus nuclei is estimated from the set of variable temperature $^{31}P\{^1H\}$ NMR spectra to be −52 °± 5 °C. Use of the Eyring equation and the expression $k_c = \pi\Delta\nu/2^{1/2}$, where k_c is the rate constant (s^{-1}) for exchange and $\Delta\nu$ is the chemical shift difference (Hz), allows the free enthalpy of activation $\Delta G^{\ddagger}$ for the exchange to be calculated.[31] This method yields $\Delta G^{\ddagger}_{221} = 38.2 \pm 0.9$ kJ/mol. The free enthalpy of activation for rotational fluxionality (an intramolecular process) has been determined for many 12-vertex metallahet-

---

(30) Green, M.; Spencer, J. L.; Stone, F. G. A.; Welch, A. J. *J. Chem. Soc., Dalton Trans.* **1975**, 179.

(31) Friebolin, H., trans. by Becconsall, J. *Basic One- and Two-Dimensional NMR Spectroscopy*, 2nd enlarged ed.; VCH: Weinheim, Germany, 1993; Chapter 11.

Table 15. Crystallographic Data for **2**, **3**, and **5**

	2	**3**	**5**
mol wt	663.91	608.90	565.12
cryst syst	monoclinic, $P2_1/n$, $Z = 4$	triclinic, $P\bar{1}$, $Z = 2$	monoclinic, $P2_1/n$, $Z = 4$
unit cell			
a (Å)	12.460(2)	11.586(3)	10.383(2)
b (Å)	11.583(2)	11.813(3)	18.875(3)
c (Å)	19.114(4)	9.799(2)	13.682(2)
α (deg)		95.33(1)	
β (deg)	107.31(1)	114.58(1)	105.41(1)
γ (deg)		80.17(1)	
V (Å^3)	2633.85	1201.31	2584.83
ϱ_{calcd} (g cm^{-3})	1.674	1.683	1.452
λ (Å)	0.710 69	0.710 69	0.710 69
μ (cm^{-1})	33.128	35.617	8.433
det−samp dist (cm)	22.5	22.5	22.5
samp-source dist (cm)	23.5	23.5	23.5
takeoff angle (deg)	2.0	2.0	2.0
av ω scan width at half-height (deg)	0.25	0.25	0.25
scan speed (deg/min)	8.0	8.0	8.0
scan width (deg)	2.0° + dispersion	2.0° + dispersion	2.0° + dispersion
single bkgd time at extremes of scan (s)	4	4	4
aperture size (mm)	3.0 × 4.0	3.0 × 4.0	3.0 × 4.0
collcn limit, 2θ (deg)	6−45	6−45	6−45
tot. no. of reflcns	3899	3323	3547
no. of unique intens	3450	3151	3368
no. with $F > 0.0$	3294	3022	3120
no. with $F > 2.33\sigma(F)$	2823	2627	2512
R for averaging	0.066	0.012	0.094
$R(F)$	0.0432	0.0235	0.0362
$R_w(F)$	0.0458	0.0245	0.0335
GOF for last cycle	1.453	1.074	0.887
max Δ/σ for last cycle	0.11	0.03	0.23

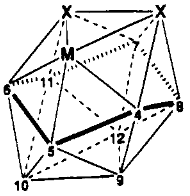

Figure 4. Icosahedral metallaheteroborane indicating long B−B distances along chair-shaped trace (thick lines).

eroboranes (mostly platinum,[18,32−35] rhodium,[36,37] and iridium[37] complexes), and these values vary widely, from 30 to 75 kJ/mol.

A second variable temperature ^{31}P{^{1}H} NMR study was done, in which excess free PMe$_2$Ph was included in the NMR sample. The results of this study are essentially the same as above, except that two other species are observed. One of these species is intermediate in nature, appearing at δ −19 ppm between 0 and −75 °C; the other remains below 0 °C, at approximately δ −5 ppm. Addition of free PMe$_2$Ph to the solution rules out a simple phosphine dissociation mechanism as the exchange process at high temperature, since dissociation is suppressed. The presence of these other species suggested to us the possibility that the complex was undergoing a *closo*/*exo-nido* tautomerism;[38] however, existence of such an *exo*−*nido* species is not clearly evident from these spectra. An interesting comparison can be made with the studies of Hawthorne et al., in which a series of

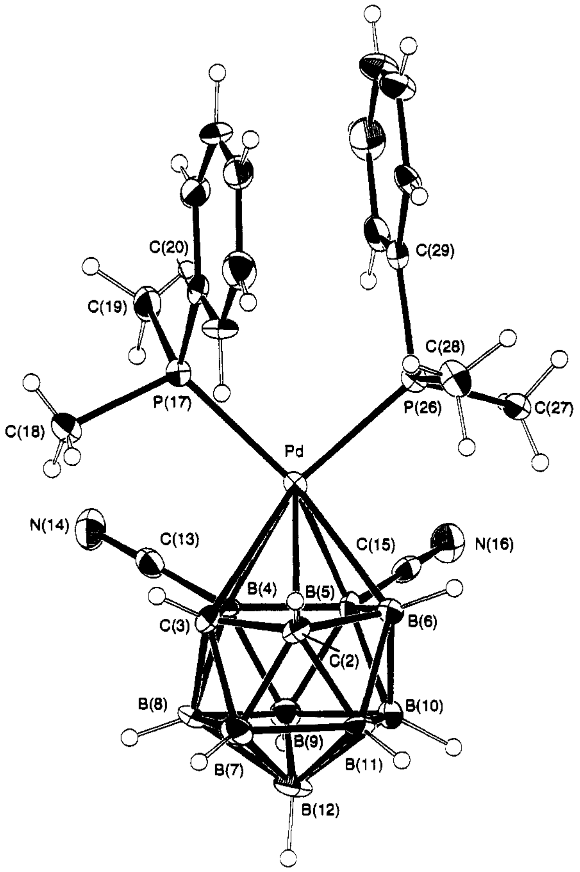

Figure 5. ORTEP diagram of 4,5-(CN)$_2$-1,1-(PMe$_2$Ph)$_2$-*closo*-1,2,3-PdC$_2$B$_9$H$_9$ (**5**).

---

(32) Stibr, B.; Jelinek, T.; Kennedy, J. D.; Fontaine, X. L. R.; Thornton-Pett, M. *J. Chem. Soc., Dalton Trans.* **1993**, 1261.

(33) Bunkhall, S. R.; Fontaine, X. L. R.; Greenwood, N. N.; Kennedy, J. D.; Thornton-Pett, M. *J. Chem. Soc., Dalton Trans.* **1990**, 73.

(34) Faridoon; Ni Dhubhghaill, O.; Spalding, T. R.; Ferguson, G.; Kaitner, B.; Fontaine, X. L. R.; Kennedy, J. D. *J. Chem. Soc., Dalton Trans.* **1989**, 1657.

(35) Ferguson, G.; Kennedy, J. D.; Fontaine, X. L. R.; Faridoon; Spalding, T. R. *J. Chem. Soc., Dalton Trans.* **1988**, 2555.

(36) Fontaine, X. L. R.; Kennedy, J. D.; McGrath, M.; Spalding, T. R. *Magn. Reson. Chem.* **1991**, 29, 711.

(37) Marder, T. B.; Baker, R. T.; Long, J. A.; Doi, J. A.; Hawthorne, M. F. *J. Am. Chem. Soc.* **1981**, 103, 2988.

(38) Baker, R. T.; Delaney, M. S.; King, R. E., III; Knobler, C. B.; Long, J. A.; Marder, T. B.; Paxson, T. E.; Teller, R. G.; Hawthorne, M. F. *J. Am. Chem. Soc.* **1984**, 106, 2965.

metallacarborane complexes $(R_3P)_2HRh(B_9H_9CRCR')$ were observed to exist in solution as *closo*, *exo-nido*, or both.[38,39] For the species existing as both *closo* and *exo−nido* in solution, subsequent crystallization showed that some species were isolable as *closo* in the solid state, and some as *exo−nido*. Thus, the species structurally determined in the solid state were not always exactly what was observed in solution. We believe that **5** similarly exhibits complex solution behavior.

The room temperature ^1H NMR of **5** indicates the cage asymmetry in that two distinct carborane proton signals are observed. However, there are only two P*Me*$_2$Ph methyl signals, whereas four should be observed according to the molecular asymmetry. The methyl signals are filled-in doublets, indicating partial virtual coupling of the phosphorus nuclei. This is consistent with the ^{31}P NMR spectrum, and the net indication of these NMR studies, then, is that the cage exists in solution at room temperature in an asymmetric environment, while the phosphines are in a less asymmetric environment, due to some complex exchange process not yet fully understood.

General Structural Observations. The X-ray structures of **A**, **2**, and **5** indicate that the P−Pd−P plane is essentially parallel to the X−X vector, where X = CH or As. This has been explained in frontier molecular orbital terms for the $[(PH_3)_2Pt]$ and $[B_9H_9(CH)_2]$ fragments.[40] However, there is significant twisting of the $(R_3P)_2Pd^{2+}$ fragment relative to the B_3X_2 face such that one R_3P is closer to the X atoms than the other (and the P−Pd−P plane is not strictly parallel to the X−X vector). This is correlated with the fact that there are two different Pd−X distances, and the longer is always on the side where the R_3P is farther from the X atoms. For example, in **5**, the P−Pd−P plane is twisted such that P(26) is further from the C−C vector than P(17) is; Pd−C(2) is 2.482 Å and Pd−C(3) is 2.332 Å. This asymmetry is consistently observed in **A**, **2**, **5**, and crystal structures of the type $(R_3P)_2M(B_9H_9X_2)$ (M = Pd,Pt; X = CH, As, Sb).[1,3,18] In **3**, the P−Pd−C plane is rotated such that the isocyanide ligand is directly over C(2). The above arguments do not apply because the frontier molecular orbitals, and thus the rotation, of the $[(^tBuNC)(PMe_2Ph)Pd]^{2+}$ fragment are presumably different from those of the $[(PMe_2Ph)_2Pd]^{2+}$ fragment.

In **A**, **2**, **3**, and **5**, of the three (As or C)−B distances for each As or C, one is short and two are long. The long bonds involve the B atoms that are bonded to two heteroatoms (Pd or As or C) rather than just one. This observation is in accord with structural details of other metallaheteroboranes.[33,34,41]

Conclusions

The organopalladium reagent $(^tBuNC)_2PdCl_2$ was used for cyano substitution on $(PMe_2Ph)_2Pd(B_9C_2H_{11})$ and $(PMe_2Ph)_2Pd(B_9H_9As_2)$ cage complexes. Substitution was observed to occur only at B(4) and/or B(5) in these palladaheteroboranes.

It is not clear what the active palladium reagent(s) is in these reactions. It is believed but not proven that the metal mediated process is generally an intermolecular process. The overall yields of products in these reactions is low, which precludes any extensive speculation about chemical pathways to the products that have been characterized.

Supporting Information Available: Tables of anisotropic thermal parameters, bond distances, and intramolecular angles (25 pages). Ordering information is given on any current masthead page.

IC9504250

---

(39) Long, J. A.; Marder, T. B.; Behnken, P. E.; Hawthorne, M. F. *J. Am. Chem. Soc.* **1984**, 106, 2979.

(40) Mingos, D. M. P.; Forsyth, M. I.; Welch, A. J. *J. Chem. Soc., Dalton Trans.* **1978**, 1363.

(41) Faridoon; Ni Dhubhghaill, O.; Spalding, T. R.; Ferguson, G.; Kaitner, B.; Fontaine, X. L. R.; Kennedy, J. D.; Reed, D. *J. Chem. Soc., Dalton Trans.* **1988**, 2739.

(42) St. Clair, D.; Zalkin, A.; Templeton, D. H. *J. Am. Chem. Soc.* **1970**, *92*, 1173.